One-hundred-million-atom electronic structure calculations on the K computer

Takeo HOSHI[1,2]

[1]*Department of Applied Mathematics and Physics, Tottori University*
Koyama Minami, Tottori 680-8550, Japan
[2] *Japan Science and Technology Agency, Core Research for Evolutional Science*
and Technology (JST-CREST), 5, Sanbancho, Chiyoda-ku, Tokyo 102-0075, Japan

Abstract

One-hundred-million atom (100-nm-scale) electronic structure calculations were realized on the K computer. The methodologies are based on inter-disciplinary collaborations among physics, mathematics and the high-performance computation field or 'Application-Algorithm-Architecture co-design'. Novel linear-algebraic algorithms were constructed as Krylov-subspace solvers for generalized shifted linear equations ($(zS - H)\boldsymbol{x} = \boldsymbol{b}$) and were implemented in our order-N calculation code 'ELSES' with modeled (tight-binding-form) systems. A high parallel efficiency was obtained with up to the full core calculations on the K computer. An application study is picked out for the nano-domain analysis of sp^2-sp^3 nano-composite carbon solid. Future aspects are discussed for next-generation or exa-scale supercomputers. The code for massive parallelism was developed with the supercomputers, the systems B and C, at ISSP.

1   Introduction

The current or next generation computational physics requires 'Application-Algorithm-Architecture co-design', or inter-disciplinary collaborations among physics, mathematics and the high-performance computation field.

Our recent papers [1, 2] report that electronic structure calculations with one-hundred-million atoms were realized on the K computer and the methodologies are based on the Application-Algorithm-Architecture co-design with novel linear algebraic algorithms [3, 4]. The calculations are called '100-nm-scale', because one hundred million atoms are those in silicon single crystal with the volume of $(126nm)^3$. The calculations were realized by our electronic structure calculation code 'ELSES' [5] and the computational cost is order-N or proportional to the number of atoms N. The code uses modelled (tight-binding-form) Hamiltonians based on *ab initio* calculations. Since the fundamental methodologies are purely mathematical, they are applicable both to insulating and metallic cases. Moreover, they are applicable also to other physics problems amang and beyond electronic structure calculations.

Fig. 1 illustrates our basic strategy for large-scale calculations with the Application-Algorithm-Architecture co-design. The essential concept is to combine new ideas among the three fields for a breakthrough. The possibility of sharing the mathematical solvers among applications will be discussed in the last section.

The present paper is organized as follows; Section 2 explains the fundamental mathematical theory. Section 3 is devoted to the computational procedures and benchmarks. Sec-
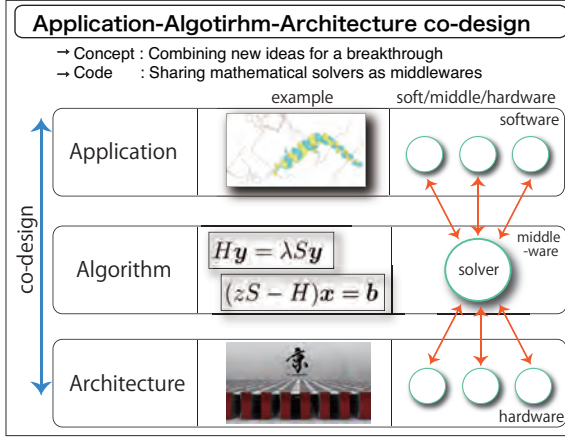
Figure 1: Application-Algorithm-Architecture co-design, our basic strategy for large-scale calculations.

tion 4 describes an application study on a nano-domain analysis of nano-composite carbon solids. Summary and future aspects are given in the last section.

2 Fundamental mathematical theory

Our fundamental mathematical theory is novel linear-algebraic algorithms with Krylov subspace.

Krylov subspace [6] is a general mathematical concept and gives the foundation of various iterative linear-algebraic solvers. such as the conjugate gradient method. A Krylov subspace is denoted as $K_\nu(A; \boldsymbol{b})$ with a given integer ν, a square matrix A and a vector $\boldsymbol{b}$, and means the linear (Hilbert) space that spanned by the ν basis vectors of $\{\boldsymbol{b}, A\boldsymbol{b}, ..., A^{\nu-1}\boldsymbol{b}\}$:

$$K_\nu(A; \boldsymbol{b}) \equiv \mathrm{span}\{\boldsymbol{b}, A\boldsymbol{b}, ..., A^{\nu-1}\boldsymbol{b}\}. \quad (1)$$

Usually, the subspace dimension ν is the iteration number of the iterative computational procedures and a matrix-vector multiplication with a vector of $\boldsymbol{v}$ ($\boldsymbol{v} \Rightarrow A\boldsymbol{v}$) governs the operation cost at each iterate.

A mathematical foundation of electronic state calculations is a generalized eigen-value equation

$$H\boldsymbol{y}_k = \varepsilon_k S\boldsymbol{y}_k. \quad (2)$$

The matrices H and S are Hamiltonian and the overlap matrices, respectively. These matrices are $M \times M$ real-symmetric (or Hermitian) matrices and S is positive definite. In this paper, the real-space atomic-orbital representation is used and the matrices are sparse real-symmetric ones. Large-matrix calculations with the conventional solvers for Eq. (2) give huge operation cost and difficulty in massive parallelism.

For years, we have constructed novel linear algebraic solvers for large-system calculations, in stead of the conventional generalized eigenvalue equation in Eq. (2). They are commonly based on linear equations in the form of

$$(zS - H)\boldsymbol{x} = \boldsymbol{b}. \quad (3)$$

Here z is a (complex) energy value and the matrix of $(zS - H)$ can be non-Hermitian. The vector $\boldsymbol{b}$ is an input and the vector $\boldsymbol{x}$ is the solution vector. The set of linear equations in Eq. (3) with many energy values is called 'generalized shifted linear equations'. A recent preprint [2] contains the complete reference list of our novel solvers and the present paper picks out two methods [7, 3].

The use of Eq. (3) results in the Green's function formalism, since the solution $\boldsymbol{x}$ of Eq. (3) is written formally as $\boldsymbol{x} = G\boldsymbol{b}$ with the Green's function $G = G(z) \equiv (zS - H)^{-1}$.

These solver algorithms are purely mathematical and applicable to large-matrix problems in many computational physics fields. Our study began for our own electronic structure calculation code and, later, grew up into more general one. For example, the shifted Conjugate Orthogonal Conjugate Gradient (sCOCG) algorithm [7], one of our algorithms, is based on a novel mathematical theorem, called collinear residual theorem [8]. After the application study on our electronic structure calculations [7], we applied

the sCOCG algorithm to a many-body problem for $La_{2-x}Sr_xNiO_4(x = 1/3, 1/2)$, since a large-matrix problem with the matrix size of 64 millions appears. [9] The sCOCG algorithms were applied also to the shell model calculation [10] and a real-space-grid DFT calculation [11]. Other applications with the collinear residual theorem [8] are found, for example, in a QCD problem [8] and a electronic excitation (GW) calculation [12].

3   Computational procedures and benchmarks

This section is devoted to the computational procedure of our electronic structure calculation and their benchmarks for the order-N scaling [3] and the parallel efficiency [1, 2]. In all the results of the present paper, the multiple Arnoldi method [3] is used as the solver for Eq. (3), since it is suitable for a molecular dynamics simulation [3]. Equation (3) is solved with the multiple Krylov subspaces of $\mathcal{L} \equiv K_p(H; \boldsymbol{b}) \oplus K_q(H; S^{-1}\boldsymbol{b})$. The subspace dimension ν is $\nu \equiv p + q$. The second term is introduced, so as to satisfy some physical conservation laws exactly. The multiple Arnoldi method gives the Green's function G.

The procedures for calculating physical quantities are briefly explained. In general, a physical quantity is defined as

$$\langle X \rangle \equiv \sum_k f(\varepsilon_k) \, \boldsymbol{y}_k^{\mathrm{T}} X \boldsymbol{y}_k \qquad (4)$$

with a given matrix X and the occupation number in the Fermi function $f(\varepsilon)$. The case in $X = H$, for example, gives the electronic structure energy

$$E_{\mathrm{elec}} \equiv \sum_k f(\varepsilon_k) \, \varepsilon_k. \qquad (5)$$

A quantity in Eq.(4) is transformed into the trace form of

$$\langle X \rangle = \mathrm{Tr}[\rho X] \qquad (6)$$

with the density matrix

$$\rho \equiv \sum_k f(\varepsilon_k) \, \boldsymbol{y}_k \, \boldsymbol{y}_k^{\mathrm{T}}. \qquad (7)$$

The density matrix is given by the Green's function as

$$\rho = \frac{-1}{\pi} \int_{-\infty}^{\infty} f(\varepsilon) \, G(\varepsilon + i0) \, d\varepsilon, \qquad (8)$$

because of

$$G(z) = \sum_k \frac{\boldsymbol{y}_k \, \boldsymbol{y}_k^{\mathrm{T}}}{z - \varepsilon_k}. \qquad (9)$$

The energy integration in Eq. (8) is carried out analytically in the multiple Arnoldi method. The chemical potential μ appears in the Fermi function $f(\varepsilon)$ and is determined by the bisection method. The computational workflow is summarized as

$$(H, S) \Rightarrow G \Rightarrow \mu \Rightarrow \rho \Rightarrow \langle X \rangle. \qquad (10)$$

Several points are discussed; (i) If the matrix X is sparse, the physical quantity $\mathrm{Tr}[\rho X] = \sum_{i,j} \rho_{ji} X_{ij}$ is contributed only from the selected elements of ρ_{ij} where $X_{ij} \neq 0$ and, therefore, we should calculate only these elements of the density matrix (ρ_{ij}) and the Green's function (G_{ij}) in the workflow of Eq. (10). The above fact is a foundation of the order-N property. (ii) The trace in Eq. (6) is decomposed into

$$\mathrm{Tr}[\rho X] = \sum_j^M \boldsymbol{e}_j^{\mathrm{T}} \rho X \boldsymbol{e}_j, \qquad (11)$$

where $\boldsymbol{e}_j \equiv (0, 0, 0, ...1_j, 0, 0, ..., 0)^{\mathrm{T}}$ is the j-th unit vector. The quantity $\boldsymbol{e}_j^{\mathrm{T}} \rho X \boldsymbol{e}_j$ is called 'projected physical quantity' and is computed in parallelism. (iii) The Green's function is used also for calculating other quantities, such as the density of states and the crystalline orbital Hamiltonian population (See the next section).

Figures 2 (a) and (b) show benchmarks. The calculated systems are amorphous-like
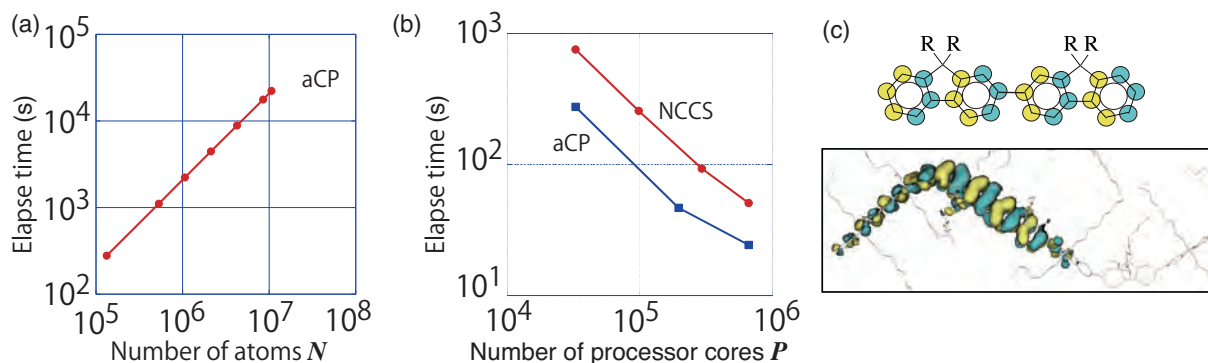
Figure 2: (a) Benchmark for the order-N scaling. [3] The calculated system is amorphous-like conjugated polymer (aCP), poly-(9,9 dioctyl fluorene). (b) Benchmark for the parallel efficiency, the 'strong scaling', on the K computer with one hundred million atoms. [1, 2] The calculated systems are aCP and an sp^2-sp^3 nano-composite carbon solid (NCCS). (c) A typical π wavefunction in aCP [1]. The upper panel is a schematic figure for two successive monomer units with $R \equiv C_8H_{17}$. The lower panel is a simulation result, where only C-C bonds are drawn for eye-guide.

conjugated polymer (aCP), poly-(9,9 dioctyl-fluorene) [3, 1, 2] and an sp^2-sp^3 nano-composite carbon solid (NCCS). [4, 1]. Figure 2(a) shows that the calculation has the order-N scaling property [3] in the aCP systems. Figure 2(b) shows the parallel efficiency on the K computer with one hundred million atoms. The MPI/OpenMP hybrid parallelism is used. The results are shown for the NCCS system with $N = 103, 219, 200$ [1] and the aCP system with $N = 102, 238, 848$ [2]. The elapse time T of the electronic structure calculation for a given atomic structure is measured as the function of the number of used processor cores P ($T = T(P)$), from $P = P_{\min} \equiv 32, 768$ to $P_{\text{all}} \equiv 663, 552$, the total number of processor cores on the K computer. The parallel efficiency is defined as $\alpha(P) \equiv T(P)/T(P_{\min})$ and such a benchmark is called 'strong scaling' in the high-performance computation field. The measured parallel efficiency among the NCCS systems is $\alpha(P = 98, 304) = 0.98$, $\alpha(P = 294, 921) = 0.90$ and $\alpha(P = P_{\text{all}}) = 0.73$. The measured parallel efficiency among the aCP systems is $\alpha(P = 196, 608) = 0.98$ and

$\alpha(P = P_{\text{all}}) = 0.56$.

The high parallel efficiency stems not only from the fundamental mathematical theory but also from detailed techniques in the high-performance computation field or the information science [4]. These techniques do not affect the numerical results. In particular, techniques were developed in (i) programing techniques for saving memory and communication costs (ii) a parallel file I/O technique, and (iii) an original visualization software called 'VisBAR' for a seamless procedure between the numerical simulation and visualization analysis (See the next section).

Physical points are briefly discussed for the calculated systems. A typical π wave function of the aCP system is shown in Fig. 2(c). The π wavefunction is terminated at the boundary region between monomer units, unlike one in an ideal chain structure, because the two monomer units are largely twisted and the π interaction between the monomer units almost vanishes. The physical property of NCCS will be discussed in the next section.

4 Nano domain analysis of nano-composite carbon solid

This section picks out an application study on nano-composite carbon solid (NCCS). A recent preprint [2] gives a review of another recent study with our code for battery-related materials [13] and earlier studies.

4.1 Analysis methods

In general, large-system calculations result in complicated nano structures with many domains and domain boundaries. Novel methods are required for the post-simulation analysis of these structures with huge electronic structure data distributed among computer nodes.

Here such analysis methods are presented with the real-space atomic-orbital representation of the Green's function; crystalline orbital Hamiltonian population (COHP) method [14], and its theoretical extension called πCOHP method [4].

The original COHP [14] is defined as

$$C_{IJ}(\varepsilon) \equiv \frac{-1}{\pi} \sum_{\alpha,\beta} H_{J\beta;I\alpha} \operatorname{Im} G_{I\alpha;J\beta}(\varepsilon + i0), (12)$$

with the atom suffixes, I and J, and the orbital suffixes, α and β. The energy integration of COHP, called ICOHP, is also defined as

$$B_{IJ} \equiv \int_{-\infty}^{\infty} f(\varepsilon) C_{IJ}(\varepsilon) d\varepsilon. \tag{13}$$

Since a large negative value of B_{IJ} ($I \neq J$) indicates the energy gain for the bond formation between the (I, J) atom pair, B_{IJ} is understood as the local bonding energy. The sum of B_{IJ} is the electronic structure energy

$$E_{\text{elec}} \equiv \sum_k f(\varepsilon_k) \varepsilon_k = \sum_{I,J} B_{IJ}. \tag{14}$$

A theoretical extension of COHP, πCOHP, is proposed [4]. Since the present Hamiltonian contains s- and p-type orbitals, off-site Hamiltonian elements are decomposed, within the Slater-Koster form, into σ and π components ($H_{J\beta;I\alpha} = H_{J\beta;I\alpha}^{(\sigma)} + H_{J\beta;I\alpha}^{(\pi)}$). From the definitions, the off-site COHP and ICOHP are also decomposed into the σ and π components

$$C_{IJ}(\varepsilon) = C_{IJ}^{(\sigma)}(\varepsilon) + C_{IJ}^{(\pi)}(\varepsilon), \quad (15)$$

$$B_{IJ} = B_{IJ}^{(\sigma)} + B_{IJ}^{(\pi)}. \tag{16}$$

The decomposed terms are called 'σ(I)COHP' and 'π(I)COHP' and the original (I)COHP is called 'full (I)COHP'.

By the σ(I)COHP and π(I)COHP, σ and π bonds can be distinguished energetically. A large negative value of $B_{IJ}^{(\sigma)}$ or $B_{IJ}^{(\pi)}$ indicates the formation of a σ or π bond between the atom pair, respectively.

The analysis method is suitable to the present massively parallel order-N method, because the full, σ, and π(I)COHP can be calculated from the Green's function without any additional inter-node data communication.

4.2 Nano domain analysis

The (π)COHP analysis method is applied to an early-stage study [4] on the formation process of the nano-polycrystalline diamond (NPD), a novel ultrahard material produced at 2003 [15]. NPD is obtained by direct conversion sintering process from graphite under high pressure and high temperature and has characteristic 10-nm-scale lamellar-like structures. NPD is of industrial importance, because of its extreme hardness and strength that exceed those of conventional single crystals. Sumitomo Electric Industries. Ltd. began commercial production from 2012. Similar properties are observed also in nano-polycrystalline SiO_2 [16].

Our simulation is motivated by the investigation of possible precursor structures in the formation process of NPD and the structures should be nano-scale composites of sp^2 (graphite-like) and sp^3 (diamond-like) domains.

Figures 3 shows the result of nano-domain analysis on sp^2-sp^3 nano-composite carbon solid (NCCS) [4]. The system is a result
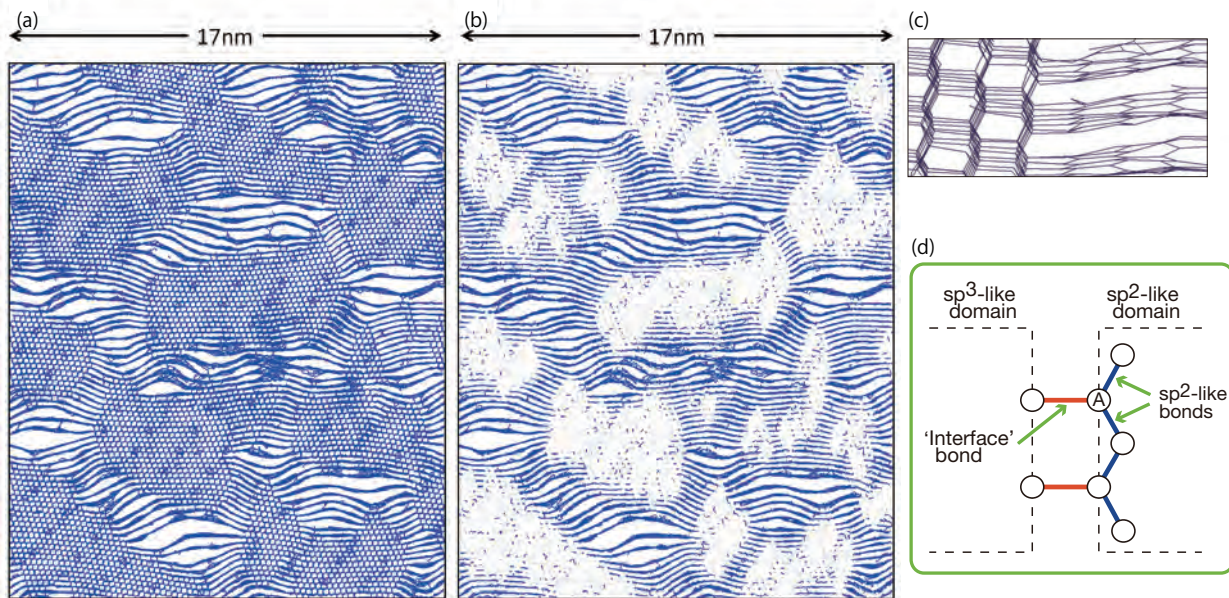
Figure 3: Nano-domain analysis of sp^2-sp^3 nano-composite carbon solid (NCCS) visualized with the COHP or πCOHP analysis [4]. The sp^2 (graphite-like) and sp^3 (diamond-like) domains are visualized in (a), while only the sp^2-like domains are visualized in (b). A closeup of a sp^2-sp^3 domain boundary is shown in (c). The atoms at a typical domain boundary are shown in (d).

of our finite-temperature molecular-dynamics simulation with a periodic boundary condition. The (π)COHP analysis is used, because sp^2 domains can be distinguished from sp^3 domains by the presence of π bonds. Figures 3(a) and (b) are drawn by the bond visualization by the full ICOHP and the πICOHP, respectively. In Fig. 3(a), a bond is drawn for an (I, J) atom pair, when its ICOHP value satisfies the condition $B_{IJ} < B_{\mathrm{th}} \equiv -9$ eV. Bond visualization by the full ICOHP indicates the visualization of both sp^2 and sp^3 bonds. In Fig. 3(b), on the other hand, a π bond is drawn, when its π ICOHP value satisfies the condition $B_{IJ}^{(\pi)} < B_{\mathrm{th}}^{(\pi)} \equiv -1.5$ eV. Bond visualization by the πICOHP indicates the visualization of only sp^2 bonds.

The analysis concludes that layered domains are sp^2 domains and non layered domains are sp^3 domains. Figure 3(c) is a close-up of a domain boundary between sp^2 and sp^3 domains, which shows that a layered domain forms a graphite-like structure and a non layered domain forms a diamond-like structure, as expected from the (π)ICOHP results.

A typical domain interface, schematically shown in Fig. 3(d), is analyzed for the nature of each bond, so as to clarify how the (π)COHP analysis works well. The atom labeled 'A' in Fig. 3(d) is focused on. The atom has three bonds that are painted blue or red in Fig. 3(d). The (π)ICOHP analysis shows that the two 'blue' bonds contain π bonds, while the 'red' bond dose not. The analysis result is consistent to the fact that the 'blue' bonds are those within an sp^2 domain, while the 'red' bond is an 'interface' bond or a bridge between sp^2 and sp^3 domains.

5 Summary and future aspects

The present paper reports our methods and results of large-scale electronic structure calculations based on our novel linear algebraic

algorithms. The mathematical algorithms are applicable to various computational physics problems among and beyond electronic structure calculations. A high parallel efficiency was observed for one-hundred-million-atom (100-nm-scale) systems with up to all the built-in cores of the K computer. An application study of nano-domain analysis on nano-composite carbon solids is shown as an example.

Finally, three future aspects are discussed; (I) Material: The present methodologies are general and an important application should be one for organic materials, since non-ideal 100-nm-scale structures are crucial for devices. Preliminary calculations are shown for amourphous-like conjugated polymers in this paper. (II) Theory: Large-system calculations for transport and optical properties should be next stages and these calculations are reduced to large-matrix problems beyond the present formulations. A central mathematical issue is the internal eigen-value problem in which we calculate only the selected eigen values and eigen vectors near the HOMO and LUMO levels or the Fermi level. Recently, a novel two-stage algorithm was proposed for the internal eigen-value problem with Sylvester's theorem of inertia [17]. (III) Code development style: As shown in Fig. 1, novel mathematical solvers can be shared as middlewares, among many application softwares or computational physics fields, because of their generality. 'Mini applications' should be also developed with the solvers, so as to clarify their mechanism and efficiency. An alpha version of such a mini application with eigen-value solvers was prepared and is now being extended [18]. Such solvers and mini applications will play a crucial role in the Application-Algorithm-Architecture co-design among next-generation or exa-scale computational physics.

Acknowledgements

References

[1] T. Hoshi, K. Yamazaki, Y. Akiyama, JPS Conf. Proc., **1** (2014) 016004.

[2] T. Hoshi, T. Sogabe, T. Miyata, D. Lee, S.-L. Zhang, H. Imachi, Y. Kawai, Y. Akiyama, K. Yamazaki and Seiya Yokoyama, Proceedings of Science, in press; Preprint : http://arxiv.org/abs/1402.7285/

[3] T. Hoshi, S. Yamamoto, T. Fujiwara, T. Sogabe, S.-L. Zhang, J. Phys.: Condens. Matter **21** (2012) 165502.

[4] T. Hoshi, Y. Akiyama, T. Tanaka and T. Ohno, J. Phys. Soc. Jpn., **82** (2013) 023710.

[5] ELSES (= Extra Large-Scale Electronic Structure calculation): http://www.elses.jp/

[6] See mathematical textbooks, such as H. A. van der Vorst *Iterative Krylov Meth-*

ods for Large Linear Systems, Cambridge Univ. Pr., (2009).

[7] R. Takayama, T. Hoshi, T. Sogabe, S.-L. Zhang, and T. Fujiwara, Phys. Rev. B **73** (2006) 165108.

[8] W. A. Frommer, Computing **70** (2003) 87; For a review, T. Sogabe and S.-L. Zhang, Bull. JSIAM **19**, 163 (2009) (in japanese).

[9] S. Yamamoto, T. Fujiwara, and Y. Hatsugai, Phys. Rev. B **76** (2007) 165114; S. Yamamoto, T. Sogabe, T. Hoshi, S.-L. Zhang and T. Fujiwara J. Phys. Soc. Jpn. **77** (2008) 114713

[10] T. Mizusaki, K Kaneko, M. Honma, T. Sakurai, Phys. Rev. C **82**, (2010) 024310.

[11] Y. Futamura, H. Tadano and T. Sakurai, JSIAM Letters **2** (2010) 127.

[12] F. Giustino, M. L. Cohen, and S. G. Louie, Phys. Rev. B **81** (2010) 115105.

[13] S. Nishino, T. Fujiwara, H. Yamasaki, S. Yamamoto, T. Hoshi, Solid State Ionics **225** (2012) 22; S. Nishino, T. Fujiwara, S. Yamamoto, and H. Yamasaki, *8th Pacific Rim International Congress on Advanced Materials and Processing*, Hawaii, 4-9. August, 2013

[14] R. Dronskowski and P. E. Blöchl: J. Phys. Chem. **97** (1993) 8617; http://www.cohp.de/

[15] T. Irifune, A. Kurio, A. Sakamoto, T. Inoue, and H. Sumiya, Nature **421** (2003) 599.

[16] N. Nishiyama, S. Seike, T. Hamaguchi, T. Irifune, M. Matsushita, M. Takahashi, H. Ohfujia and Y. Kono, Scripta Materialia **67** (2012) 955.

[17] D. Lee, T. Miyata, T. Sogabe, T. Hoshi, S.-L. Zhang, Japan J. Indust.

Appl. Math. **30**, (2013) 6255; in *International Workshop on Eigenvalue Problems: Algorithms; Software and Applications, in Petascale Computing (EPASA2014)*, Tsukuba-city, Japan, 7-9, Mar. 2014.

[18] http://www.damp.tottori-u.ac.jp/~hoshi/eigen_test/; T. Hoshi, H. Imachi, Y. Kawai, Y. Akiyama, K. Yamazaki, S. Yokoyama, in *International Workshop on Eigenvalue Problems: Algorithms; Software and Applications, in Petascale Computing (EPASA2014)*, Tsukuba-city, Japan, 7-9, Mar. 2014.